Am J Transl Res 2026;18(4):3408-3423
www.ajtr.org /ISSN:1943-8141/AJTR0172007

Original Article

FAM19A5 is an independent prognostic biomarker in thyroid cancer

Shoujing Luan[1,2], Haiqing Yuan[3], Deshan Liu[1]

[1]Department of Traditional Chinese Medicine, Qilu Hospital of Shandong University, Jinan 250012, Shandong, China; [2]Department of Metabolic Diseases and Weight Management, The First Affiliated Hospital of Shandong Second Medical University, Weifang 261041, Shandong, China; [3]Intensive Care Unit, The First Affiliated Hospital of Shandong Second Medical University, Weifang 261041, Shandong, China

Received February 10, 2026; Accepted April 19, 2026; Epub April 25, 2026; Published April 30, 2026

Abstract: Objectives: Family with sequence similarity 19 member A5 (FAM19A5), also known as TAFA chemokine-like family member 5 (TAFA5), has been implicated in tumorigenesis. This study aimed to investigate the role of FAM19A5 in thyroid cancer (TC) using bioinformatics analysis and *in vitro* functional assays. Methods: RNA sequencing (RNA-seq) data and clinicopathologic characteristics of 513 patients with papillary thyroid cancer (PTC) were retrieved from the Cancer Genome Atlas (TCGA) database and re-analyzed. The diagnostic performance of FAM19A5 was evaluated using receiver operating characteristic (ROC) curve analysis. The Kaplan-Meier method was used to analyze overall survival (OS) and disease-specific survival (DSS). Cox regression analysis was performed to identify independent risk factors for PTC. Gene set enrichment analysis (GSEA) was applied to explore signaling pathways associated with FAM19A5. The mRNA expression of FAM19A5 was detected by quantitative real-time PCR (RT-qPCR). Cell proliferation, migration, and invasion were assessed using colony formation, wound healing, and Transwell assays, respectively. Protein expression of FAM19A5 and nuclear factor kappa B (NF-κB) pathway-related proteins was detected by Western blot. Results: FAM19A5 expression was significantly upregulated in TC tissues and cells. Elevated FAM19A5 expression was correlated with advanced T stage, lymph-node metastasis, and poorer OS and DSS. GSEA showed enrichment of NF-κB signaling pathways in tumors with high FAM19A5 high-expression. FAM19A5 knockdown significantly inhibited TC cell proliferation, migration, and invasion. Furthermore, treatment with tumor necrosis factor alpha (TNF-α), an activator of NF-κB, reversed the inhibitory effects induced by FAM19A5 knockdown. Conclusions: FAM19A5 is an independent predictor of poor prognosis in TC and may serve as a potential therapeutic target. Mechanistically, FAM19A5 knockdown suppresses TC cell proliferation, migration, and invasion, potentially through modulation of the NF-κB pathway.

Keywords: FAM19A5, thyroid cancer, prognosis, NF-κB pathway

Introduction

Thyroid cancer (TC) is a malignant tumor of the thyroid gland, and its incidence and detection rates have steadily increased in recent years [1]. Most TC cases originate from follicular epithelial cells, including follicular TC, papillary thyroid cancer (PTC), and undifferentiated anaplastic TC [2-4]. Although most patients have a favorable prognosis, a small proportion may develop aggressive disease characterized by extra-thyroidal extension, lymph node metastasis, and recurrence, often accompanied by treatment resistance [5, 6]. Therefore, the identification of reliable molecular biomarkers that reflect tumor invasiveness and guide targeted therapy is of great clinical importance.

Family with sequence similarity 19 member A5 (FAM19A5), also known as TAFA chemokine-like family member 5 (TAFA5), has recently been reported to function as a novel adipokine with vascular protective effects [7-10]. FAM19A5 is highly expressed in the central nervous system and is involved in neurodevelopment, as well as in neurological disorders such as brain injury and optic neuritis [9, 11, 12]. Furthermore, aberrant expression of FAM19A5 has been observed in tumors such as glioma, gastric cancer (GC), and mantle cell lymphoma (MCL)

https://doi.org/10.62347/ZLIJ9407

[13-16]. These findings suggest that FAM19A5 may play a role in tumorigenesis across various malignancies, potentially through shared molecular mechanisms.

Although progress has been made in understanding the role of FAM19A5 in cancer, its function in TC remains unclear. Therefore, elucidating the role of FAM19A5 in TC may provide novel insights into its clinical diagnosis and management. This study aimed to evaluate the diagnostic and prognostic value of FAM19A5 in PTC, explore its potential biological functions through bioinformatics analysis and in vitro experiments, and elucidate its mechanism of action, particularly its association with NF-κB signaling pathway. This study may provide a theoretical basis for improving the diagnosis and treatment of TC.

Materials and methods

Data acquisition and preprocessing

RNA sequencing (RNA-seq) expression profiles and corresponding clinical data of PTC patients were retrieved from The Cancer Genome Atlas (TCGA) database via a genomic data-sharing portal. A total of 513 tumor tissues and 59 normal thyroid tissues were initially collected. After applying the inclusion criteria, 486 samples (including case and control groups) were retained for subsequent analysis. The expression data were normalized to transcripts per million (TPM), and genes with low expression levels were excluded (TPM <1 in more than 80% of the samples).

Differential expression and receiver operating characteristic (ROC) curve analysis

Differentially expressed genes (DEGs) were identified using the *edgeR* software package (version 3.42.0). Genes with |log2-fold changes| >1 and a false discovery rate (FDR) <0.05 were considered significantly differentially expressed. The diagnostic performance of FAM19A5 was evaluated using ROC curve analysis.

Clinical relevance and survival analysis

The association between FAM19A5 expression and clinical features was analyzed. Overall survival (OS) and disease-specific survival (DSS) were assessed using Kaplan-Meier survival analysis. A multivariate Cox proportional hazards regression model was constructed to evaluate independent prognostic factors, adjusting for potential confounding factors such as age, stage, and lymph node status.

Gene set enrichment analysis (GSEA)

Gene set enrichment analysis (GSEA) was performed to explore potential molecular signaling pathways associated with FAM19A5 expression. The clusterProfiler R package (version 4.6.2) was used, and gene sets were obtained from the Molecular Signatures Database (MSigDB). Tumor samples were divided into high- and low-expression groups according to the median expression level of FAM19A5. Significantly enriched pathways were defined as those with an FDR <0.25 and a nominal *p*-value <0.05.

Cell culture and siRNA transfection

Normal human thyroid epithelial cells (Nthy-ori3-1) and TC cell lines (TPC-1, CAL62, and SW579) were obtained from Yaji Biological (Shanghai, China). Cells were cultured in RPMI 1640 medium supplemented with 10% fetal bovine serum (FBS; Beyotime, China) at 37°C in 5% CO_2. Small interfering RNA (siRNA) targeting FAM19A5 (si-FAM19A5) and a scrambled control (si-NC) were purchased from GemmaPharma (Shanghai, China). Transfection was performed using the Lipofectamine 3000 kit (Thermo Fisher Scientific, USA) according to the manufacturer's instructions. Cells were seeded in 6-well plates at a density of 1×10^6 cells per well and allowed to reach 70%-80% confluence prior to transfection. Briefly, 5 μL of Lipofectamine 3000 reagent was diluted in 200 μL of optimal minimal essential medium (Opti-MEM), while 5 μL of 20 μM si-FAM19A5 or si-NC was diluted separately in 200 μL of Opti-MEM. After incubation at room temperature for 5 min, the two solutions were gently mixed and further incubated at room temperature for 20 min to allow complex formation. The mixture was then added to the cells cultured in Opti-MEM, followed by gentle mixing. After 6 h of incubation, the medium was replaced with complete culture medium. After 24 to 48 h of incubation, the cells were collected for subsequent mRNA or protein expression analysis.

The si-FAM19A5 sequences targeting FAM19A5 were as follow: Forward: 5'-GCUGCGACUUGUUAAUCAATT-3', Reverse: 5'-UUGAUUAACAAGUCGCAGCTT-3'.

Quantitative real-time PCR (RT-qPCR)

Total RNA was extracted using Trizol reagent (Vazyme, China) according to the manufacturer's instructions. Complementary DNA (cDNA) was synthesized using a PrimeScript RT kit (Thermo Fisher Scientific). RT-qPCR was performed on a LightCycler 480 system (Roche, Switzerland) using SYBR Green Master Mix (Takara, Japan). β-actin was used as an internal control. Relative gene expression levels were calculated using the $2^{-\Delta\Delta Ct}$ method.

Primers sequences were as follows: FAM19A5, Forward: 5'-GACATGCTTCCGTGTCTGGA-3', Reverse: 5'-GTGGTCTTTATCCTCCCGCC-3'. β-actin, Forward: 5'-GAAGAGCTACGAGCTGCCTGA-3', Reverse: 5'-CAGACAGCACTGTGTTGGCG-3'.

Western blot

Total protein was extracted using RIPA lysis buffer (Beyotime, China) according to the manufacturer's instructions. Protein concentration was measured using a bicinchoninic acid (BCA) assay kit (Beyotime, China). Equal amounts of protein were separated by sodium dodecyl sulfate polyacrylamide gel electrophoresis (SDS-PAGE) and then transferred onto polyvinylidene fluoride (PVDF) membranes (Epizyme, China). After blocking with 5% skimmed milk for 1 h at room temperature, the membranes were incubated overnight at 4°C with primary antibodies against FAM19A5 (Thermo Fisher Scientific, 1:1000), NF-κB p65 (Abcam, 1:1000), p-NF-κB p65 (Abcam, 1:1000), and β-actin (Abcam, 1:1000). Subsequently, the membranes were incubated with horseradish peroxidase (HRP)-conjugated secondary antibodies anti-mouse or anti-rabbit immunoglobulin G (IgG; Thermo Fisher Scientific) at room temperature for 1 h. Protein bands were visualized using an enhanced chemiluminescence (ECL) detection system (Beyotime, China), and band intensities were quantified using ImageJ software (National Institutes of Health, USA).

Clone formation assay

Cells were seeded into 6-well plates at a density of 1×10^3 cells per well and cultured at 37°C in a humidified incubator with 5% CO_2. The culture medium was replaced every 3 days. After 14 days of incubation, cells were fixed with 4% paraformaldehyde (Beyotime, China) and stained with 1% crystal violet solution for 15 min. The staining solution was then discarded, and the wells were gently rinsed with phosphate-buffered saline (PBS), air-dried, and photographed. Colonies consisting of ≥50 cells were counted to assess clonogenic capacity.

Wound healing assay

A sterile 10 μL pipette tip was used to create linear scratches on the cell monolayer. The cells were washed with PBS buffer to remove detached cells. Scratch images were captured at 0, 24 and 48 h to wound closure. Wound width was measured using Image J software (NIH, USA), and cell migration was evaluated based on the wound closure rate. The wound healing rate (%) was calculated as follows: (initial wound width - wound width at indicated time point)/initial wound width ×100%.

Transwell migration and invasion assay

Cell migration and invasion assays were performed using Transwell chambers (Corning, USA). For the invasion assay, the upper chamber was pre-coated with Matrigel (BD Biosciences, USA), whereas no Matrigel was used for the migration assay. A total of 5×10^3 cells suspended in serum-free medium were seeded into the upper chamber. The lower chamber was filled with medium containing 10% FBS as a chemoattractant. After incubation for 24-48 h, non-invading cells on the upper surface were carefully removed. Cells that migrated or invaded to the lower surface were fixed with 4% paraformaldehyde, stained with crystal violet, and subsequently imaged and counted under a light microscope.

Statistical analysis

All statistical analyses were performed using GraphPad Prism 5.0 software (GraphPad Software, USA). Data are presented as mean ± standard deviation. Comparisons between two groups were performed using Student's *t*-test. Comparisons among multiple groups were conducted using one-way or repeated-measures analysis of variance (ANOVA), followed by Tukey's post hoc Test. Categorical variables

Table 1. Baseline data of thyroid cancer (TC) patients in TCGA database

Characteristics	Numbers of cases (n (%)
Age	
<50	286 (55.75)
≥50	227 (44.25)
Gender	
Female	373 (72.71)
Male	140 (27.29)
Histological_type	
NA	9 (1.75)
Classical/usual	366 (71.35)
Follicular	102 (19.88)
Tall	36 (7.02)
Stage	
NA	2 (0.39)
I	289 (56.34)
II	52 (10.14)
III	113 (22.03)
IV	57 (11.11)
T_classification	
T1	143 (27.88)
T2	169 (32.94)
T3	176 (34.31)
T4	23 (4.48)
TX	2 (0.39)
N_classification	
N0	230 (44.83)
N1	233 (45.42)
NX	50 (9.75)
M_classification	
NA	1 (0.19)
M0	286 (55.75)
M1	9 (1.75)
MX	217 (42.3)
Radiation_therapy	
NA	20 (3.9)
No	178 (34.7)
Yes	315 (61.4)
Residual_tumor	
NA	32 (6.24)
R0	393 (76.61)
R1	54 (10.53)
R2	4 (0.78)
RX	30 (5.85)
Vital_status	
Deceased	16 (3.12)
Living	497 (96.88)
Sample_type	
Metastatic	8 (1.56)
Primary tumor	505 (98.44)
FAM19A5	
High	78 (15.2)
Low	435 (84.8)

were analyzed using the chi-square test. Cox proportional hazards regression analysis was used to evaluate prognostic risk factors. Receiver operating characteristic (ROC) curve analysis was performed to assess the diagnostic significance of FAM19A5 expression. A P value <0.05 was considered statistically significant.

Results

FAM19A5 was upregulated in TC and correlated with tumor aggressiveness

Analysis of TCGA database (**Table 1**) showed that FAM19A5 expression was significantly upregulated in PTC tissues compared with normal thyroid tissue (FDR <0.001) (**Figure 1A**). Subgroup analysis of FAM19A5 expression across different PTC subtypes (**Figure 1B**, **1C**), stage (**Figure 1D**), T classification (**Figure 1E**), N classification (**Figure 1F**), M classification (**Figure 1G**), age (**Figure 1H**), gender (**Figure 1I**), radiation therapy (**Figure 1J**), residual tumor (**Figure 1K**), and vital status (**Figure 1L**) are shown in **Figure 1.** Notably, elevated FAM19A5 expression was significantly associated with histological type, tumor stage, T_classification, M_Classification, and vital status, but not with sex, age, or history of radiation therapy (**Figure 1C-L**) (**Table 2**).

Diagnostic and prognostic significance of FAM19A5 in TC

ROC curve analysis demonstrated that FAM19A5 had high diagnostic accuracy across different TNM stages, with the area under the curve (AUC) exceeding 0.9, indicating excellent diagnostic performance (**Figure 2A-E**). Kaplan-Meier survival analysis showed that patients with high FAM19A5 expression had significantly shorter OS, and this association remained consistent in subgroup analyses stratified by age and tumor stage (**Figure 3**). After adjusting for age, T stage, and N stage, FAM19A5 remained

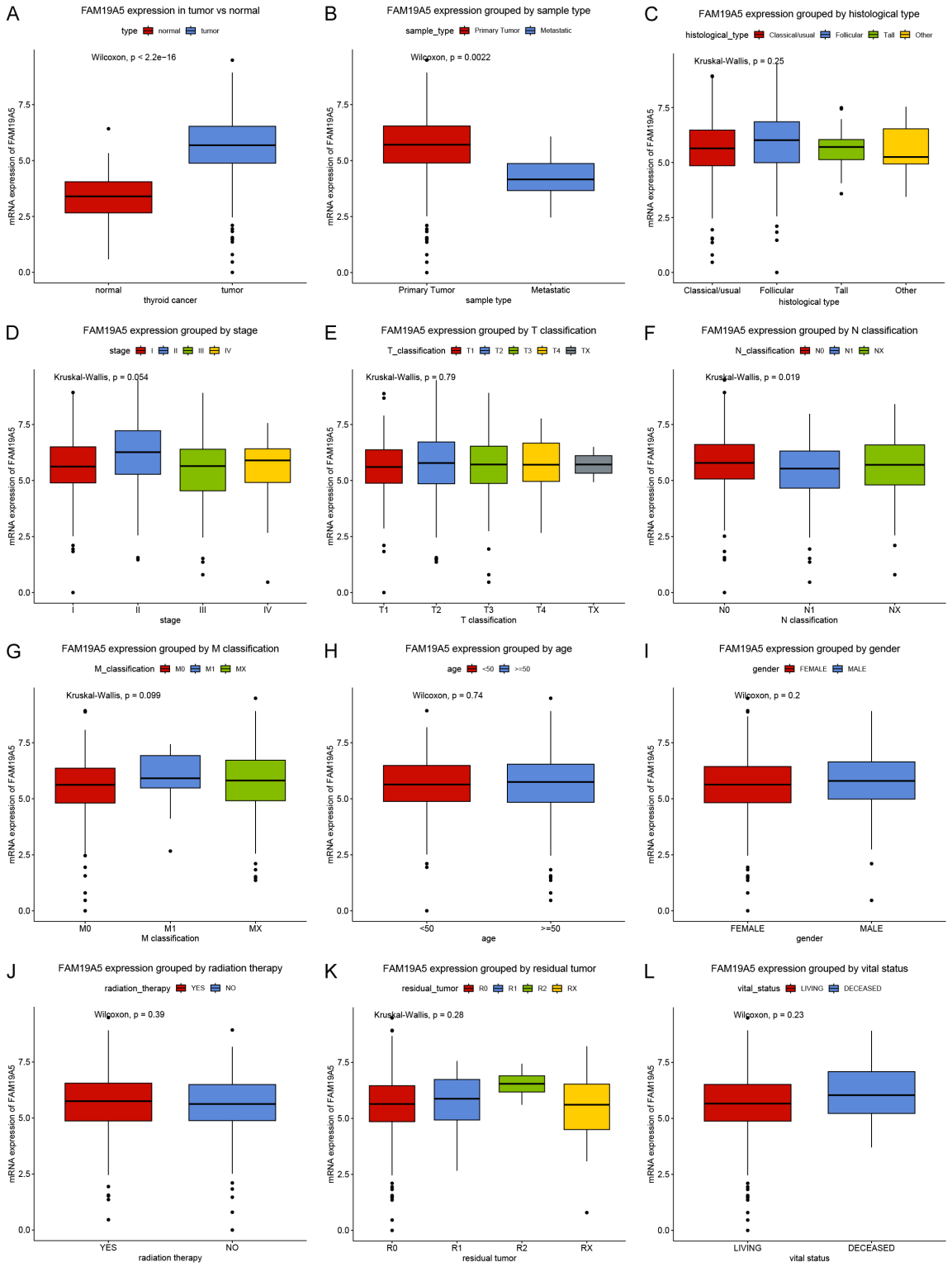

Figure 1. Family with sequence similarity 19, member A5 (FAM19A5) expression in thyroid cancer (TC). A. Boxplot showing FAM19A5 mRNA expression in thyroid carcinoma versus normal thyroid tissue. B-L. Stratified expression analysis of FAM19A5 was conducted according to sample type, histologic type, tumor stage, T classification, N classification, M classification, age, gender, radiation therapy, residual tumor, and vital status.

Table 2. The association between FAM19A5 expression and clinicopathological parameters

Parameter	Variable	N	FAM19A5 mRNA expression				χ^2	*P* value
			High	%	Low	%		
Age	<50	286	42	(53.85)	244	(56.09)	0.060	0.807
	≥50	227	36	(46.15)	191	(43.91)		
Gender	Female	373	52	(66.67)	321	(73.79)	1.353	0.245
	Male	140	26	(33.33)	114	(26.21)		
Histological_type	Classical/usual	366	49	(63.64)	317	(74.24)	9.068	0.011
	Follicular	102	25	(32.47)	77	(18.03)		
	Tall	36	3	(3.9)	33	(7.73)		
Stage	I	289	37	(47.44)	252	(58.2)	11.090	0.020
	II	52	16	(20.51)	36	(8.31)		
	III	113	17	(21.79)	96	(22.17)		
	IV	57	8	(10.26)	49	(11.32)		
T_classification	T1	143	14	(17.95)	129	(29.66)	11.594	0.019
	T2	169	36	(46.15)	133	(30.57)		
	T3	176	22	(28.21)	154	(35.4)		
	T4	23	6	(7.69)	17	(3.91)		
	TX	2	0	(0)	2	(0.46)		
N_classification	N0	230	38	(48.72)	192	(44.14)	1.265	0.490
	N1	233	31	(39.74)	202	(46.44)		
	NX	50	9	(11.54)	41	(9.43)		
M_classification	M0	286	33	(42.31)	253	(58.29)	8.161	0.014
	M1	9	3	(3.85)	6	(1.38)		
	MX	217	42	(53.85)	175	(40.32)		
Radiation_therapy	No	178	22	(29.33)	156	(37.32)	1.429	0.232
	Yes	315	53	(70.67)	262	(62.68)		
Residual_tumor	R0	393	54	(75)	339	(82.89)	2.617	0.319
	R1	54	11	(15.28)	43	(10.51)		
	R2	4	1	(1.39)	3	(0.73)		
	RX	30	6	(8.33)	24	(5.87)		
Vital_status	Deceased	16	6	(7.69)	10	(2.3)	4.708	0.030
	Living	497	72	(92.31)	425	(97.7)		
Sample_type	Metastatic	8	0	(0)	8	(1.84)	0.505	0.477
	Primary tumor	505	78	(100)	427	(98.16)		

an independent predictor of poor OS (**Table 3**). Additionally, elevated FAM19A5 expression was associated with poorer DSS (**Figure 4**; **Table 4**).

FAM19A5-associated pathways in TC

GSEA revealed that high FAM19A5 expression was significantly enriched in multiple biological pathways, including metabolism, Alzheimers disease pathway, and vascular smooth muscle contraction pathway (**Table 5**). The normalized enrichment score (NES) for the nuclear factor kappa B (NF-κB) signaling pathway was 1.98 (FDR = 0.005) (**Figure 5A-C**). These findings suggest that FAM19A5 may be involved in metabolic reprogramming and inflammatory signaling in PTC.

FAM19A5 was highly expressed, and its silencing inhibited NF-κB pathway activation in TC cells

To explore the role of FAM19A5 in TC, its expression levels were first examined in TC cell lines. The results showed that FAM19A5 was highly expressed in TC cells compared with normal thyroid cells (**Figure 6A-C**). Based on the GSEA results, FAM19A5 expression was closely associated with the NF-κB pathway.

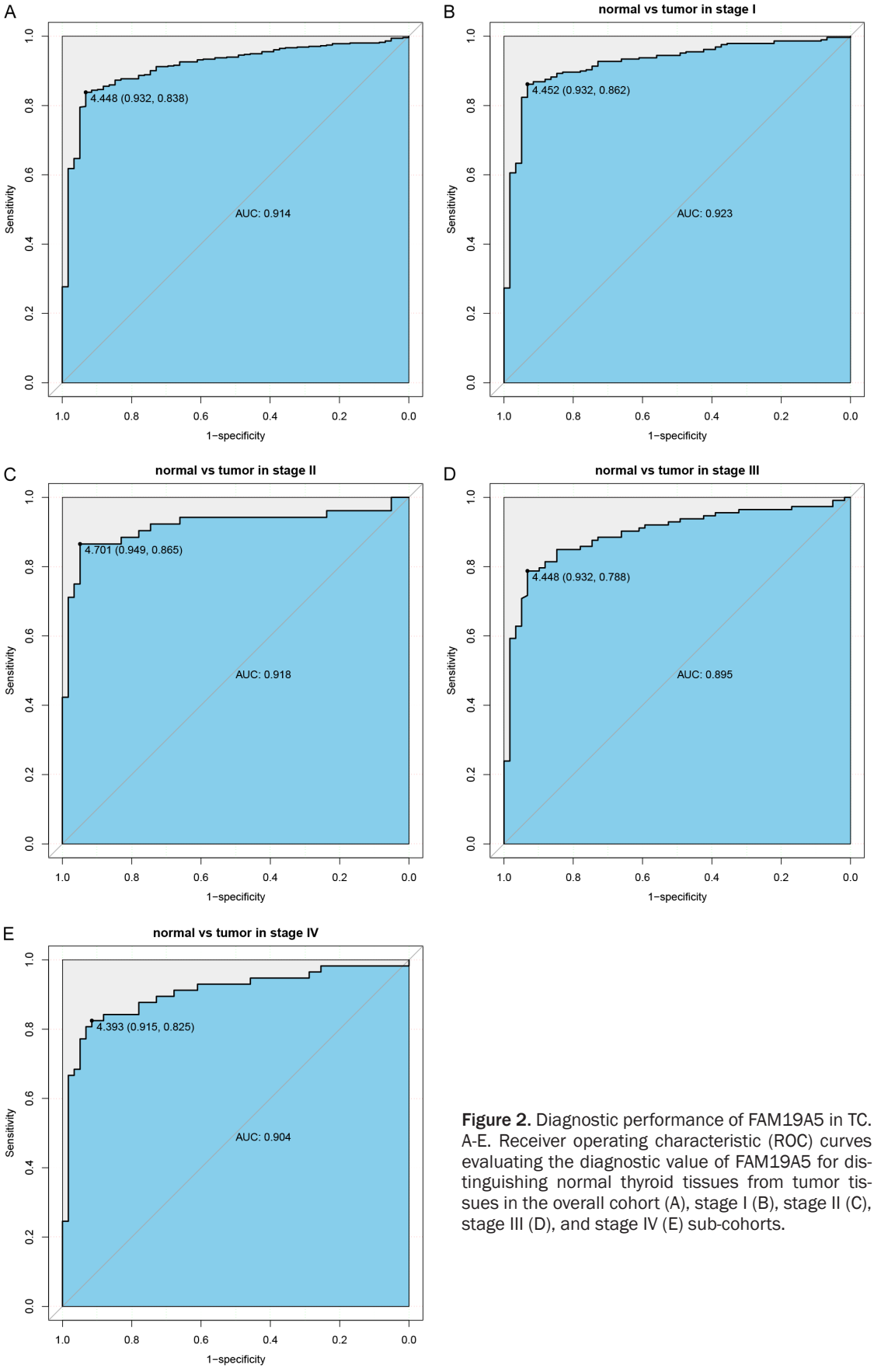

Figure 2. Diagnostic performance of FAM19A5 in TC. A-E. Receiver operating characteristic (ROC) curves evaluating the diagnostic value of FAM19A5 for distinguishing normal thyroid tissues from tumor tissues in the overall cohort (A), stage I (B), stage II (C), stage III (D), and stage IV (E) sub-cohorts.

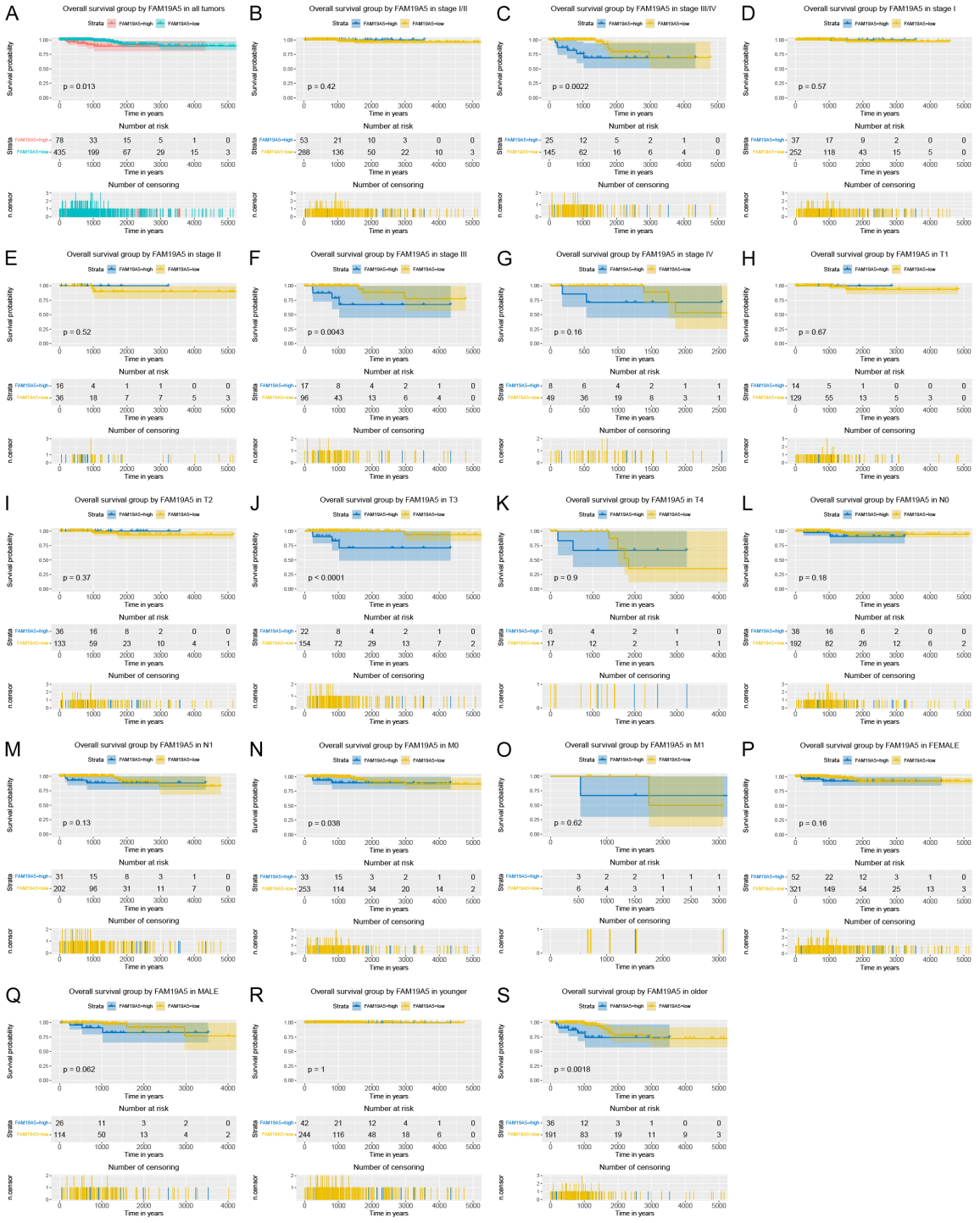

Figure 3. Kaplan-Meier survival analysis of overall survival (OS) based on FAM19A5 expression in TC. A-S. Kaplan-Meier curves comparing OS between high and low FAM19A5 expression groups in the following subgroups: overall cohort, stage I/II, stage III/IV, stage I, stage II, stage III, stage IV, T1, T2, T3, T4, N0, N1, M0, M1, female, male, younger, and older subgroups.

To further investigate this relationship, the effects of FAM19A5 on NF-κB pathway activation were assessed. The TPC-1 cell line, which exhibited the highest FAM19A5 expression, was selected for subsequent knockdown experiments using siRNA. FAM19A5 expression was

Table 3. Univariate and multivariate analysis of factors associated with overall survival (OS)

Parameters	Univariate analysis			Multivariate analysis		
	Hazard Ratio	95% CI	*P* value	Hazard Ratio	95% CI	*P* value
Age	1.2E+09	0-Inf	0.997			
Gender	1.98	0.72-5.47	0.189			
Histological_type	0.4	0.12-1.38	0.147			
Stage	2.53	1.59-4.05	0.000	2.12	1.22-3.67	0.007
T_classification	2.61	1.4-4.86	0.003	1.31	0.68-2.51	0.423
N_classification	0.91	0.44-1.86	0.793			
M_classification	2.12	0.86-5.23	0.104			
Radiation_therapy	0.62	0.26-1.5	0.293			
Residual_tumor	1.67	1.1-2.54	0.016	1.25	0.77-2.03	0.374
FAM19A5	3.36	1.22-9.25	0.019	2.93	1.06-8.11	0.039

Table 4. Univariate and multivariate analysis of factors associated with disease-specific survival (DSS)

Parameters	Univariate analysis			Multivariate analysis		
	Hazard Ratio	95% CI	*P* value	Hazard Ratio	95% CI	*P* value
Age	1.1E+09	0-Inf	0.998			
Gender	4.07	0.9-18.33	0.067			
Histological_type	0.27	0.04-1.82	0.177			
Stage	4.19	1.67-10.48	0.002	2.7	0.96-7.58	0.06
T_classification	7.36	2.25-24.07	0.001	2.66	0.79-8.91	0.114
N_classification	0.64	0.22-1.83	0.408			
M_classification	2.54	0.65-9.98	0.182			
Radiation_therapy	1.4	0.29-6.69	0.676			
Residual_tumor	1.78	0.99-3.22	0.056			
FAM19A5	7.4	1.65-33.12	0.009	6.5	1.44-29.48	0.015

Table 5. Gene set in high FAM19A5 patients

Name	SIZE	ES	NES	NOM *p*-value
KEGG_NITROGEN_METABOLISM	23	-0.60217	-1.53977	0.012766
KEGG_ALZHEIMERS_DISEASE	157	-0.38693	-1.53467	0.043222
KEGG_VASCULAR_SMOOTH_MUSCLE_CONTRACTION	114	-0.48842	-1.49213	0.041575

significantly decreased after si-FAM19A5 transfection (**Figure 6D-F**). Notably, phosphorylated NF-κB P65 was also significantly decreased following FAM19A5 knockdown (**Figure 6G**, **6H**).

Silencing FAM19A5 suppresses the malignant phenotypes of TPC-1 cells

To further evaluate the functional role of FAM19A5 in TC progression, a series of in vitro assays were performed. FAM19A5 knockdown significantly inhibited the proliferation, migration, and invasion of TPC-1 cells (**Figure 7**).

NF-κB pathway activation reverses the effects of FAM19A5 knockdown in TPC-1 cells

To further investigate whether FAM19A5 regulates the biological behavior of TC cells through the NF-κB pathway, rescue experiments were conducted. After si-FAM19A5 transfection, cells were treated with TNF-α, a known activator of the NF-κB pathway. Compared with the si-NC group, si-FAM19A5 group exhibited markedly suppressed colony formation, migration, and invasion in TPC-1 cells. However, treatment with TNF-α partially reversed these inhibitory effects (**Figure 8**).

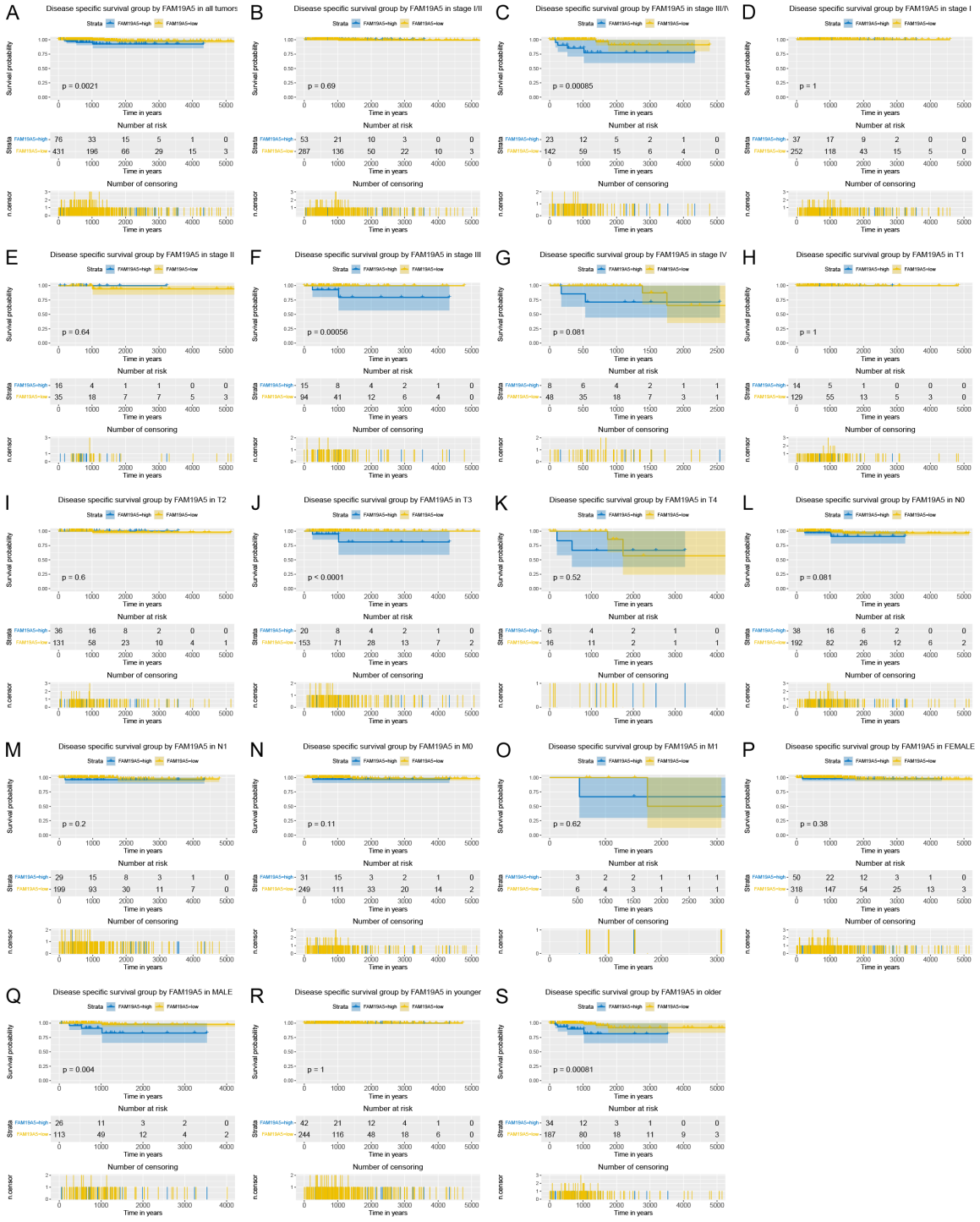

Figure 4. Kaplan-Meier analysis of disease free survival (DSS) in TC. A-S. Kaplan-Meier curves comparing DSS between high and low FAM19A5 expression groups in the following subgroups: overall cohort, stage I/II, stage III/IV, stage I, stage II, stage III, stage IV, T1, T2, T3, T4, N0, N1, M0, M1, female, male, younger, and older subgroups.

Discussion

In the present study, integrated transcriptome analysis showed that FAM19A5 was significantly upregulated in PTC and was associated with an unfavorable prognosis. Functional validation further demonstrated that FAM19A5 may be involved in the regulation of NF-κB pathway and promotes tumor cell migration, invasion, and clone formation in PTC cells.

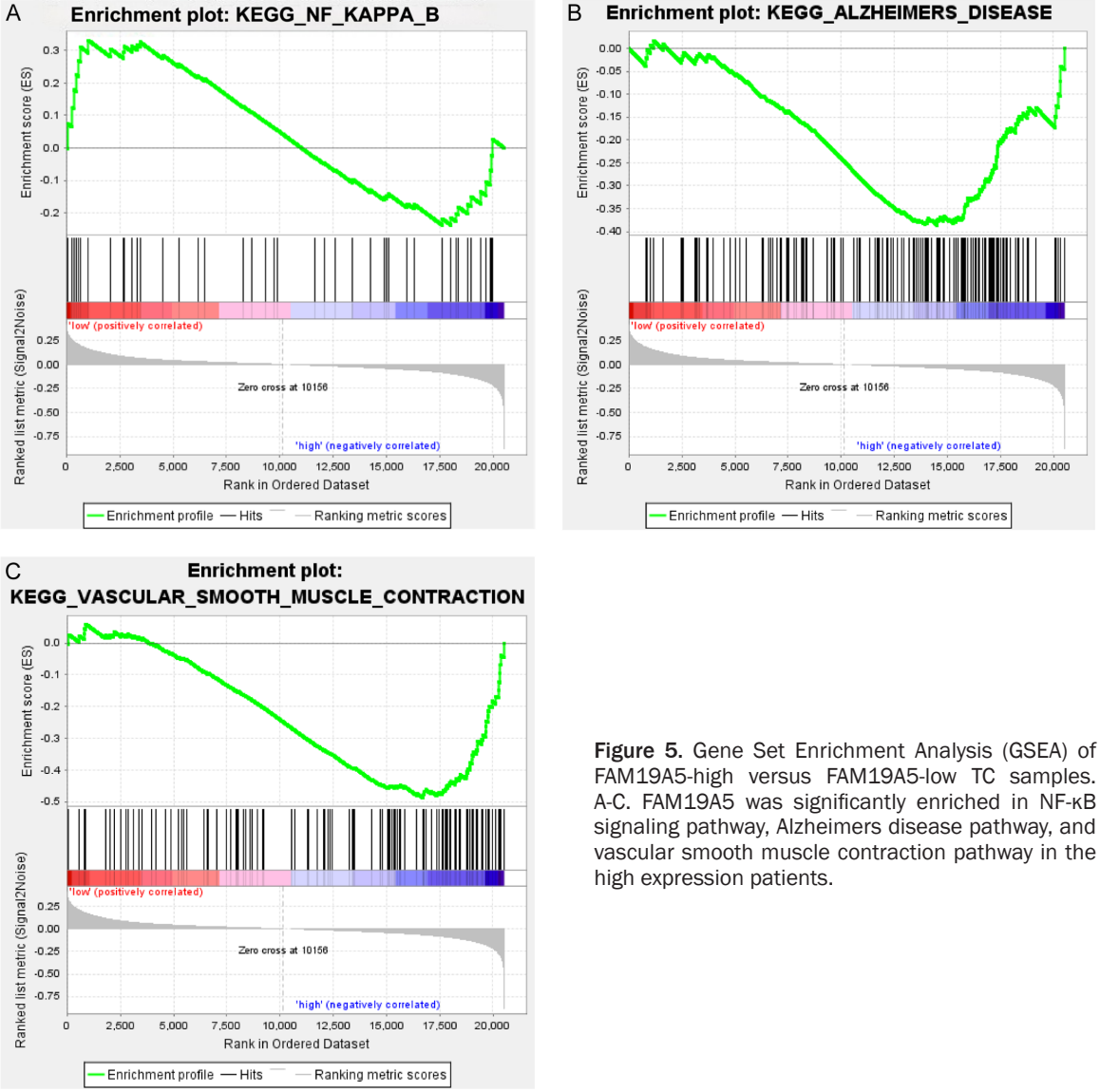

Figure 5. Gene Set Enrichment Analysis (GSEA) of FAM19A5-high versus FAM19A5-low TC samples. A-C. FAM19A5 was significantly enriched in NF-κB signaling pathway, Alzheimers disease pathway, and vascular smooth muscle contraction pathway in the high expression patients.

Our database analysis indicated that elevated FAM19A5 expression was significantly associated with aggressive clinicopathological features, including advanced T stage and lymph node metastasis. Both univariate and multivariate Cox regression analyses identified FAM19A5 as an independent prognostic factor in PTC. These findings are consistent with previous studies. For instance, FAM19A5 has been reported to be highly expressed in gastric cancer (GC), where its upregulation is associated with poor patient prognosis [14]. Similarly, in mantle cell lymphoma (MCL), patients with high FAM19A5 expression had significantly shorter progression-free survival, suggesting its potential as a prognostic biomarker [16]. Moreover, FAM19A5 knockdown has been shown to inhibit malignant behaviors in GC and MCL cells [14, 15]. In line with these observations, our in vitro experiments demonstrated that FAM19A5 knockdown significantly inhibited TPC-1 cell proliferation, invasion, and migration. Collectively, FAM19A5 could serve as a potential biomarker for the clinical diagnosis and prognosis assessment of TC.

The NF-κB pathway is closely associated with multiple processes related to tumorigenesis, including tumor initiation, growth, and metastasis [17]. In this study, GSEA demonstrated that high FAM19A5 expression was significantly associated with NF-κB pathway. The NF-κB

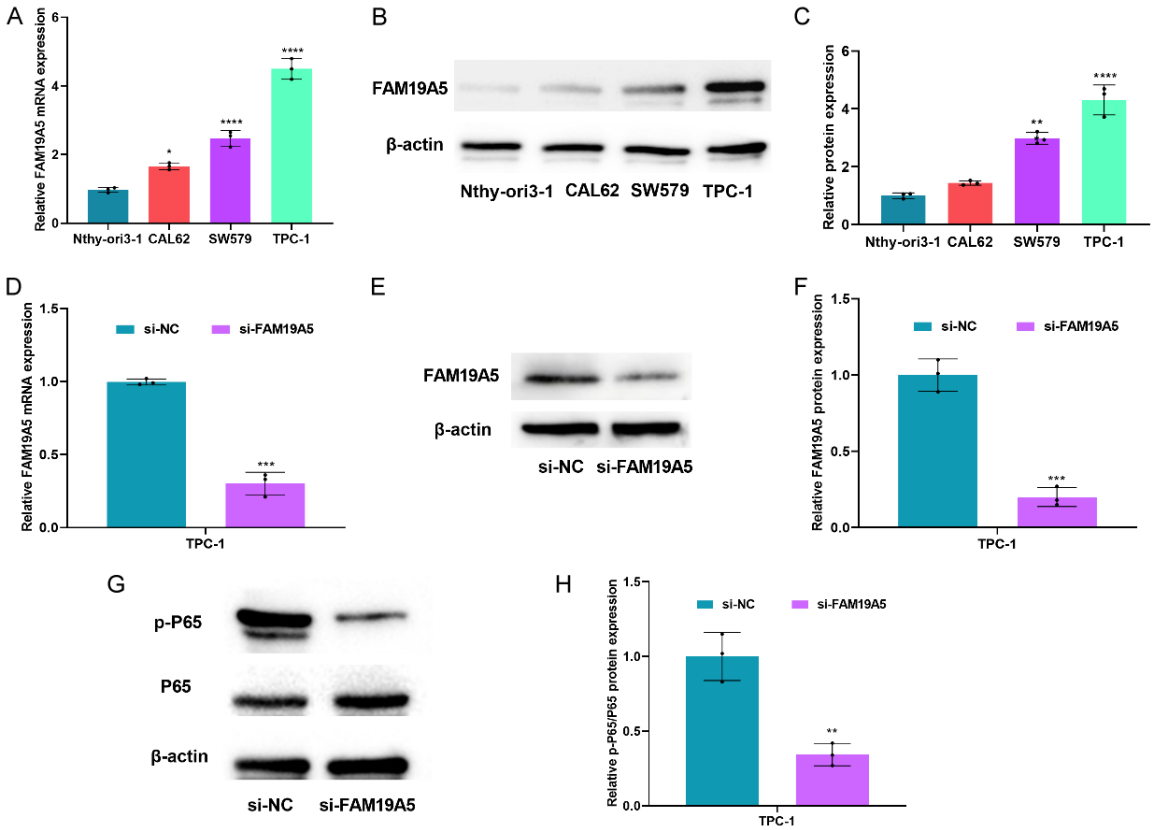

Figure 6. Silencing FAM19A5 inhibited NF-κB signaling in TC cells. A. Relative mRNA expression of FAM19A5 in TC cells and normal thyroid cells. B, C. Protein expression of FAM19A5 in TC cells and normal thyroid cells. D. Relative mRNA expression of FAM19A5 in TPC-1 cells after transfection. E, F. Protein expression of FAM19A5 in TPC-1 cells after transfection. G, H. Protein levels of P65 and p-P65 in TPC-1 cells after transfection. **P*<0.05, ***P*<0.01, ****P*<0.001, *****P*<0.0001, compared to the Nthy-ori3-1 or si-NC group.

pathway is a key inflammation-related carcinogenic signaling pathway that promotes angiogenesis and cell proliferation and is constitutively activated in various human cancers [18]. NF-κB p65 is a central subunit of the NF-κB complex and plays critical roles in multiple biological processes, including cell proliferation and tumorigenesis [19]. Aberrant phosphorylation of P65 can directly lead to dysregulation of the NF-κB pathway, thereby contributing to the development of various diseases, including cancer [18, 20-22]. In thyroid cells, abnormal activation of NF-κB, induced by factors such as chronic inflammation, can inhibit apoptosis, promote cell proliferation, accelerate cell invasion and metastasis, and enhance resistance to radiotherapy and chemotherapy, ultimately facilitating TC progression [23]. The NF-κB pathway acts as a critical regulator of malignant progression in TC by driving abnormal cell proliferation, inhibiting apoptosis, enhancing invasion and metastasis, and modulating the tumor immune microenvironment [24]. Therefore, inhibitors targeting this pathway have been proposed as potential therapeutic strategies for TC [25]. However, due to its structural complexity, functional diversity, and multilayered regulation, further investigation is warranted to elucidate the upstream regulatory mechanisms and downstream effectors of NF-κB signaling in TC.

Based on these findings, functional assays were conducted to explore the relationship between FAM19A5 and NF-κB in PTC. The results showed that FAM19A5 knockdown significantly decreased the phosphorylation level of P65 in TPC-1 cells, suggesting that FAM19A5 may be involved in regulating NF-κB pathway activation. To further determine whether FAM19A regulates malignant behaviors of TPC-1 cells through NF-κB pathway, rescue

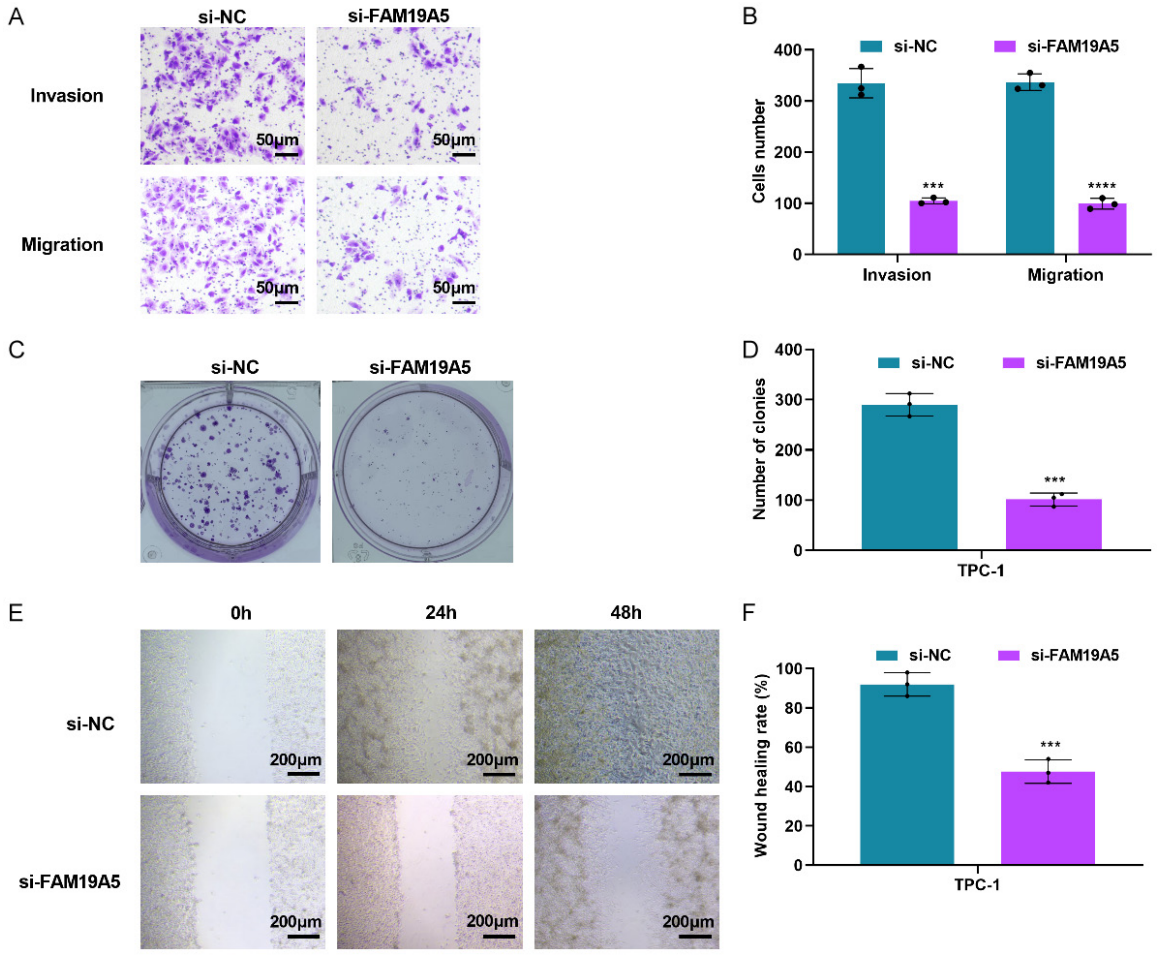

Figure 7. FAM19A5 knockdown suppressed the malignant biological behaviors of TPC-1 cells. A, B. Transwell assays showing that FAM19A5 knockdown significantly inhibited the invasion and migration abilities of TPC-1 cells (magnification: 200×). C, D. Colony formation assays demonstrating that FAM19A5 knockdown reduced the clonogenic ability of TPC-1 cells. E, F. Wound healing assays indicating that FAM19A5 knockdown suppressed the migratory ability of TPC-1 cells (magnification: 100×). ***P<0.001, ****P<0.0001, compared to the si-NC group.

experiments using TNF-α (an NF-κB activator) were performed. The results demonstrated that TNF-α treatment counteracted the inhibitory effects of FAM19A5 knockdown on the malignant behaviors of TPC-1 cells. These findings suggest that FAM19A5 may promote TC progression, at least partially, through modulation of the NF-κB pathway.

These findings provide support for the potential of targeting the FAM19A5-NF-κB axis as a therapeutic strategy in TC. From a clinical perspective, elevated FAM19A5 expression may serve as a biomarker to improve risk stratification in TC patients. However, several limitations of this study should be acknowledged. First, this study was based on TCGA data, which may be subject to selection bias and lacks treatment-related information, such as radioactive iodine dosage. Second, the present study did not fully elucidate the specific molecular mechanisms by which FAM19A5 regulates the NF-κB pathway in TC cells, and further mechanistic investigations are warranted. Third, although the functional role of FAM19A5 was validated in cell lines, further validation in multiple PTC cell lines and *in vivo* xenograft models is required to enhance the generalizability of the findings. In addition, the upstream and downstream regulatory mechanisms underlying the upregulation of FAM19A5 remain unclear. For instance, whether FAM19A5 is regulated by lncRNAs or miRNAs requires further investigation in TC. In this study, GSEA results also indicated that high FAM19A5 expression was associated with

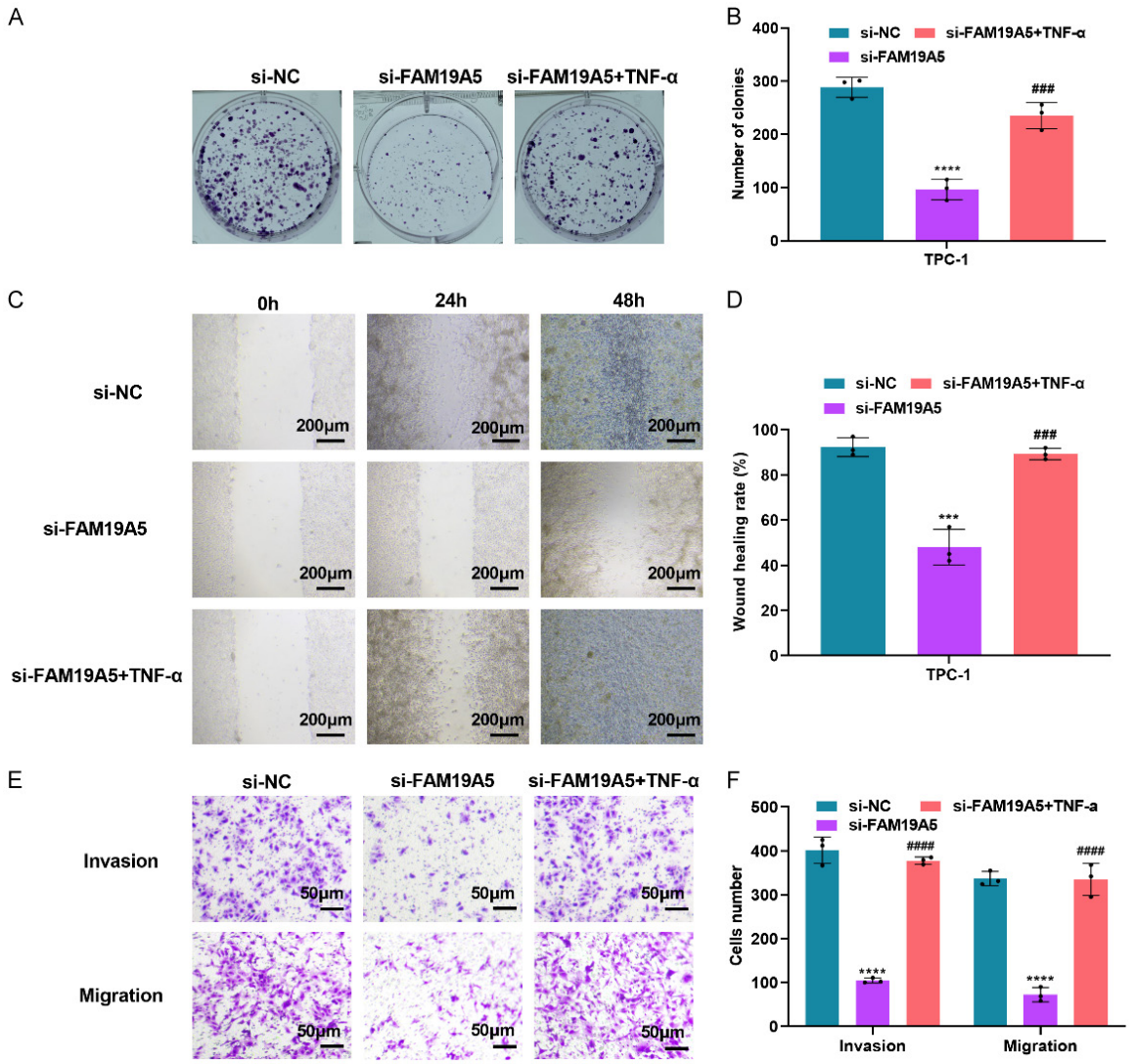

Figure 8. Effects of FAM19A5 knockdown and NF-κB pathway activation on TPC-1 cell behaviors. A, B. Clone formation assay showing the clone formation ability in FAM19A5-silencing TPC-1 cells with or without TNF-α treatment. C, D. Wound healing assay showing the migratory ability of FAM19A5-silencing TPC-1 cells with or without TNF-α treatment (magnification: 100×). E, F. Transwell assay evaluating migration and invasion in FAM19A5-silencing TPC-1 cells with or without TNF-α treatment (magnification: 200×). ***P<0.001, ****P<0.0001, compared to the si-NC group. ###P<0.001, ####P<0.0001, compared to the si-FAM19A5 group.

pathways related to fatty acid metabolism and cholesterol homeostasis. Future studies should therefore focus on validating the role of FAM19A5 in metabolic reprogramming using both in *vitro* and in *vivo* models and elucidating the underlying molecular mechanisms linking FAM19A5 to metabolic regulation in TC. Furthermore, prospective multicenter cohort studies with comprehensive molecular characterization are needed to determine whether FAM19A5 can serve as a predictive biomarker for novel metabolic or immune-targeted therapies in TC.

Conclusion

FAM19A5 is upregulated in TC and is an independent prognostic factor in PTC. FAM19A knockdown suppresses malignant phenotypes of TC cells, potentially through modulation of the NF-κB pathway. These findings suggest that FAM19A5 may serve as a promising biomarker and a potential therapeutic target in TC.

Disclosure of conflict of interest

None.

Address correspondence to: Deshan Liu, Department of Traditional Chinese Medicine, Qilu Hospital of Shandong University, Jinan 250012, Shandong, China. E-mail: liudeshan@sdu.edu.cn

References

[1] Grimm D. Recent advances in thyroid cancer research. Int J Mol Sci 2022; 23: 4631.

[2] Boucai L, Zafereo M and Cabanillas ME. Thyroid cancer: a review. JAMA 2024; 331: 425-435.

[3] Chen DW and Haymart MR. Unravelling the rise in thyroid cancer incidence and addressing overdiagnosis. Nat Rev Endocrinol 2026; 22: 10-20.

[4] Miranda-Filho A, Lortet-Tieulent J, Bray F, Cao B, Franceschi S, Vaccarella S and Dal Maso L. Thyroid cancer incidence trends by histology in 25 countries: a population-based study. Lancet Diabetes Endocrinol 2021; 9: 225-234.

[5] Leboulleux S, Boucai L, Busaidy N, Durante C, Fagin JA, Fazeli S, Gianoukakis AG, Haugen BR, Kang H, Konda B, Laetsch TW, Locati L, Ryder M, Spitzweg C, Worden FP, Wirth L and Ho A. Redifferentiation therapy in unresectable or metastatic radioactive iodine refractory thyroid cancer: an International Thyroid Oncology Group statement. Lancet Diabetes Endocrinol 2025; 13: 516-527.

[6] Haddad RI, Bischoff L, Applewhite M, Bernet V, Blomain E, Brito M, Busaidy NL, Campbell M, DeLozier O, Duh QY, Ehya H, Grady E, Guo T, Haymart M, Hunt JP, Kandeel F, Kotwal A, Lamonica DM, Lorch J, Mandel SJ, Markovina S, Mydlarz W, Nabell L, Raeburn CD, Rezaee R, Ridge JA, Ritter H, Roth MY, Salgado SA, Scheri RP, Shah JP, Sipos JA, Sippel R, Sturgeon C, Wirth LJ, Wong RJ, Worden F, Yeh MW, Darlow S, Cassara CJ and Sliker B. NCCN Guidelines® Insights: Thyroid Carcinoma, Version 1.2025. J Natl Compr Canc Netw 2025; 23: e250033.

[7] Zheng J, He J and Li H. FAM19A5 in vascular aging and osteoporosis: mechanisms and the "calcification paradox". Ageing Res Rev 2024; 99: 102361.

[8] Yari FA, Shabani P, Karami S, Sarmadi N, Poustchi H and Bandegi AR. Circulating levels of FAM19A5 are inversely associated with subclinical atherosclerosis in non-alcoholic fatty liver disease. BMC Endocr Disord 2021; 21: 153.

[9] Lee YB, Hwang HJ, Kim JA, Hwang SY, Roh E, Hong SH, Choi KM, Baik SH and Yoo HJ. Association of serum FAM19A5 with metabolic and vascular risk factors in human subjects with or without type 2 diabetes. Diab Vasc Dis Res 2019; 16: 530-538.

[10] Huang S, Zheng C, Xie G, Song Z, Wang P, Bai Y, Chen D, Zhang Y, Lv P, Liang W, She S, Li Q, Liu Z, Wang Y, Xing GG and Wang Y. FAM19A5/TAFA5, a novel neurokine, plays a crucial role in depressive-like and spatial memory-related behaviors in mice. Mol Psychiatry 2021; 26: 2363-2379.

[11] Shahapal A, Cho EB, Yong HJ, Jeong I, Kwak H, Lee JK, Kim W, Kim B, Park HC, Lee WS, Kim H, Hwang JI and Seong JY. FAM19A5 expression during embryogenesis and in the adult traumatic brain of FAM19A5-LacZ knock-in mice. Front Neurosci 2019; 13: 917.

[12] Kang D, Kim HR, Kim KK, Kim DH, Jeong B, Jin S, Park JW, Seong JY and Lee BJ. Brain-specific chemokine FAM19A5 induces hypothalamic inflammation. Biochem Biophys Res Commun 2020; 523: 829-834.

[13] Díaz de Ståhl T, Hartmann C, De Bustos C, Piotrowski A, Benetkiewicz M, Mantripragada KK, Tykwinski T, Von Deimling A and Dumanski JP. Chromosome 22 tiling-path array-CGH analysis identifies germ-line- and tumor-specific aberrations in patients with glioblastoma multiforme. Genes Chromosomes Cancer 2005; 44: 161-169.

[14] Hu Z, Niu G, Ren J, Wang X, Chen L, Hong R and Ke C. TAFA5 promotes proliferation and migration in gastric cancer. Mol Med Rep 2019; 20: 4477-4488.

[15] Wang Y, Zhang Z, Wan W, Liu Y, Jing H and Dong F. FAM19A5/S1PR1 signaling pathway regulates the viability and proliferation of mantle cell lymphoma. J Recept Signal Transduct Res 2022; 42: 225-229.

[16] Wang Y, Huang S, Zhang Z, Dong F, Wang Y, Jing H and Ke X. Expression of FAM19A5 in mantle cell lymphoma patients and its clinical significance. J Exp Hematol 2020; 28: 1183-1188.

[17] Mao H, Zhao X and Sun SC. NF-κB in inflammation and cancer. Cell Mol Immunol 2025; 22: 811-839.

[18] Yu H, Lin L, Zhang Z, Zhang H and Hu H. Targeting NF-κB pathway for the therapy of diseases: mechanism and clinical study. Signal Transduct Target Ther 2020; 5: 209.

[19] Viatour P, Merville MP, Bours V and Chariot A. Phosphorylation of NF-κB and IκB proteins: implications in cancer and inflammation. Trends Biochem Sci 2005; 30: 43-52.

[20] Pradère JP, Hernandez C, Koppe C, Friedman RA, Luedde T and Schwabe RF. Negative regulation of NF-κB p65 activity by serine 536 phosphorylation. Sci Signal 2016; 9: ra85.

[21] Jiang C, Zhang C, Dai M, Wang F, Xu S, Han D, Wang Y, Cao Y, Liang Y, Zhang Z, Yan L, Shen Y, He K, Shen Y and Liu J. Interplay between SUMO1-related SUMOylation and phosphoryla-

tion of p65 promotes hepatocellular carcinoma progression. Biochim Biophys Acta Mol Cell Res 2024; 1871: 119595.
[22] Guo Q, Jin Y, Chen X, Ye X, Shen X, Lin M, Zeng C, Zhou T and Zhang J. NF-κB in biology and targeted therapy: new insights and translational implications. Signal Transduct Target Ther 2024; 9: 53.
[23] Song Y and Liu C. Research progress on NF-κB and thyroid cancer. J Practical Medicine 2014; 30: 3673-3674.
[24] Crescenzi E, Leonardi A and Pacifico F. NF-κB in thyroid cancer: an update. Int J Mol Sci 2024; 25: 11464.
[25] Li X, Abdel-Mageed AB, Mondal D and Kandil E. The nuclear factor kappa-B signaling pathway as a therapeutic target against thyroid cancers. Thyroid 2013; 23: 209-218.